Single Inductor DC-DC Converter with Bipolar Outputs using Charge Pump

Kenji Takahashi*, Hajime Yokoo*, Shunsuke Miwa*, Kengo Tsushida*, Hiroyuki Iwase*, Kazuki Murakami*,
Nobukazu Takai*, Haruo Kobayashi*, Takahiro Odaguchi†, Shigeki Takayama†, Isao Fukai† and Jun-ichi Matsuda†

* Graduate School of Electrical Engineering
Faculty of Engineering
Gunma University, Gunma, Japan 378–8515

† Asahi Kasei Toko Power Devices Corporation

***Abstract*—This paper describes a bipolar outputs DC-DC converter that uses a single inductor for size and cost reduction. We propose timing diagram for a charge pump circuit in the negative voltage generation part, and present its configuration, operation principle and simulation results. We also show that employing pseudo-continuous conduction mode improves cross-regulation between the two outputs.**

I. Introduction

Portable devices such as cellular phones, PDA's, game appliances, and so on, have become a large and lucrative market for switching power IC's. Switching regulator is suitable for the power supply circuit of the mobile equipment because of its high efficiency, small size, and low power consumption characteristics. Low cost, high efficiency and extremely small system solutions are critical to success, but the demands are quite conflicting.

The active matrix Organic Electro Luminescence (AMOEL) display is a strong candidate for mobile applications owing to its high resolution, low power consumption and low cost. AMOEL panels, however, usually require bipolar power supplies with different regulated voltages. Therefore, boost switching converters that can supply bipolar outputs for this application are important.

Single-inductor multiple-output (SIMO) switching converters can support more than one output while requiring only one off-chip inductor, which yields many appealing advantages for mass-production and applications. The SIMO boost switching converter is reported in [1]–[4]. The SIMO converter works in pseudo-continuous conduction mode (PCCM) with a freewheel period, trying to handle large load currents and eliminate cross-regulation [5]–[7]. PCCM technique is suitable for SIMO converter because of its advantage for cross-regulation.

In [1], SIMO switching converter with bipolar outputs using charge pump, is proposed. However the negative output voltage of [1] depends on its positive output voltage. This feature restricts application field for bipolar outputs converter.

In this paper, single inductor DC-DC converter with bipolar outputs is proposed. In order to realize independence of each output voltage, we propose new timing diagram of the conventional circuitry. The bipolar outputs of the converter can vary its output voltage by duty ratio independently. Simulations are performed to verify the proposed method. Simulation results of transient analysis by Spectre program indicate that the positive output voltage is constant for variation of the negative output voltage using the proposed timing diagram while the negative output voltage depends on the positive output voltage using the conventional timing diagram. Simulation results also indicate cross-regulation characteristic is good performance for the proposed method.

II. SIMO DC-DC Converter

A. Circuit schema and conventional timing diagram

Figure 1(a) indicates single-inductor multiple-output switching converter [1]. The switching converter of Fig. 1(a) consists of a boost converter, a charge pump, and a freewheel switch. The converter can supply bipolar outputs by using conventional timing diagram of Fig. 1(a). The conventional timing diagram is composed of three regions i.e. "stage 1," "stage 2," and "stage 3" as shown in Fig.1(b). In order to find bipolar outputs of the converter, circuit equations of each region are given as follows.

1) region "stage 1": Only switch S_1 turns on, so inductor L stores energy from voltage source V_{in}. Relations between inductor current i_L, the input voltage V_{in}, and positive output voltage V_{op} are found as

$$\frac{d}{dt}i_L = \frac{V_{in}}{L}, \tag{1}$$
$$\frac{d}{dt}V_{op} = -\frac{V_{op}}{R_{op}C_{op}}. \tag{2}$$

2) region "stage 2": Only switch S_2 turns on, so the inductor L supplies its energy to output terminal of V_{op} and charges C_{op}. Thus relations between i_L, V_{in}, and V_{op} become

$$\frac{d}{dt}i_L = \frac{V_{in} - V_{op}}{L}, \tag{3}$$
$$\frac{d}{dt}V_{op} = \frac{i_L}{C_{op}} - \frac{V_{op}}{R_{op}C_{op}}. \tag{4}$$

In this phase, because both switch S_2 and S_3 turn on, the voltage of C_c becomes V_{op}.

978-1-4244-7456-4/10/$26.00

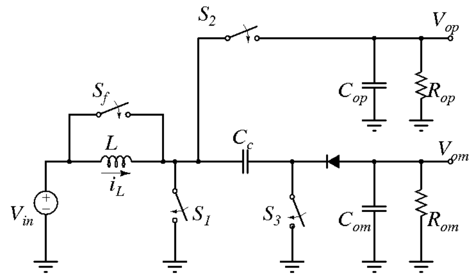

(a) SIMO DC-DC converter schematic [1].

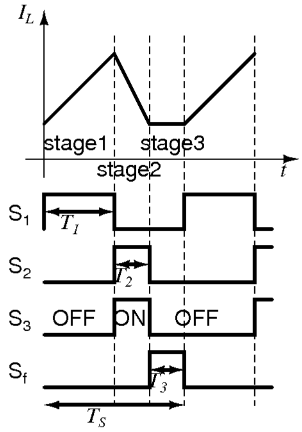

(b) Conventional timing diagram.

Fig. 1. Single inductor bipolar outputs DC-DC converter with charge pump.

3) region "stage 3": Freewheel switch S_f turns on and the inductor L keeps its energy and realize PCCM.

4) region "stage 1(next phase)": Because switch S_1 turns on and the voltage of C_c is V_{op}, the negative output voltage V_{om} is given by:

$$V_{om} = -V_{op} + V_F, \tag{5}$$

where V_F is diode drop voltage. Eq.(5) shows that the negative output voltage depends on the positive output voltage.

From Eq.(1)–Eq.(4), we can get state-space averaging equation as

$$\frac{d}{dt}\begin{pmatrix} i_L \\ V_{op} \end{pmatrix} = \begin{pmatrix} 0 & -\frac{D_2}{L} \\ \frac{D_2}{C_{op}} & -\frac{D_1+D_2}{R_{op}C_{op}} \end{pmatrix} \begin{pmatrix} i_L \\ V_{op} \end{pmatrix} + \begin{pmatrix} \frac{D_1+D_2}{L} \\ 0 \end{pmatrix} V_{in}, \tag{6}$$

where D_1 and D_2 are duty ratio of "stage 1" and "stage 2" i.e. T_1/T_s and T_2/T_s, respectively. From the stage-space averaging equation, the positive output voltage V_{op} is found as

$$V_{op} = \frac{D_1 + D_2}{D_2} V_{in}. \tag{7}$$

Eq.(7) indicates that the conventional timing diagram can control V_{op} with the duty ratio D_1 and D_2, however Eq. (5) shows V_{om} is dependent of V_{op}. These results restrict the application field of Fig.1(a).

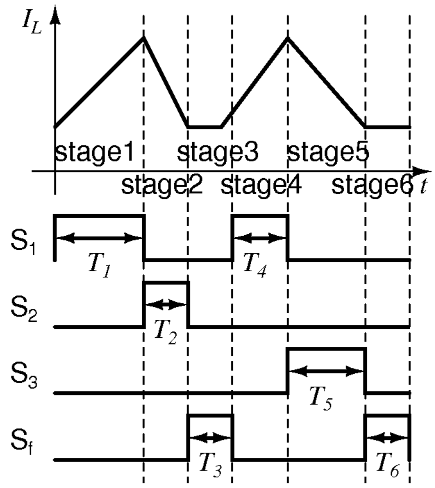

Fig. 2. Proposed timing diagram.

In next section, we propose new timing diagram which the negative output voltage is independent of the positive output voltage.

B. Proposed timing diagram

Figure 2 indicates proposed timing diagram. The proposed timing diagram has 6 stages and is applied to the same circuit of Fig.1(a). The timing diagram is separated into two phases, i.e. one phase for the positive voltage, the other for the negative voltage. The "stage 1" and "stage 2" determine the positive output voltage, and the "stage 4" and "stage 5" the negative output voltage, respectively. Circuit equations of each region are given as follows.

1) "stage 1"∼ "stage 3": In these stages, analysis is performed in the same way as subsection II-A, and the same equations are obtained. Thus state-space averaging equation for V_{op} becomes the same and V_{op} is obtained as Eq.7.

2) "stage 4": Because only switch S_1 turns on, inductor L stores energy from voltage source V_{in} again. Relations between inductor current i_L, the input voltage V_{in}, and negative output voltage V_{om} are given as

$$\frac{d}{dt} i_L = \frac{V_{in}}{L}, \tag{8}$$

$$\frac{d}{dt} V_{om} = \frac{i_L}{C_{om}} - \frac{V_{om}}{R_{om}C_{om}}. \tag{9}$$

3) "stage 5": Since switch S_3 turns on, charge pump capacitor C_c charges energy from the inductor L. Thus relations between i_L, V_{in}, and V_{op} becomes

$$\frac{d}{dt} i_L = \frac{V_{in} - V_{om}}{L}, \tag{10}$$

$$\frac{d}{dt} V_{om} = -\frac{V_{om}}{R_{om}C_{om}}. \tag{11}$$

4) "stage 6": Freewheel switch S_f turns on and the inductor L keeps its energy. From Eq.(8)–Eq.(11), state-space

TABLE I
SIMULATION CONDITIONS

Input voltage V_{in}	3.5V
switching frequency	500kHz
inductor	2μH
output capacitance C_{op}, C_{om}	10μF
load resistance	15Ω
charge pump capacitance C_c	5μF
on resistance	$10\text{m}\Omega$
diode drop voltage	0.85V

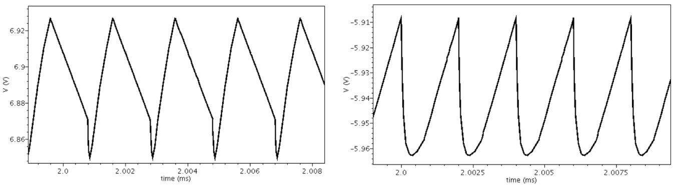

Positive output voltage. Negative output voltage.

(a) Simulation results under condition 1.

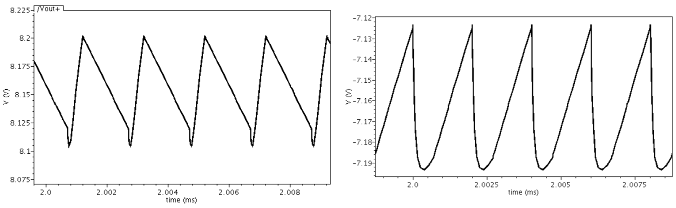

Positive output voltage. Negative output voltage.

(b) Simulation results under condition 2.

Fig. 3. Transient responses using the conventional timing diagram.

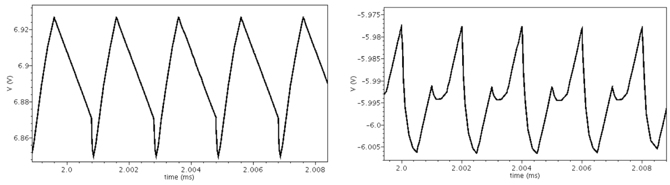

Positive output voltage. Negative output voltage.

(a) Simulation results under condition 3.

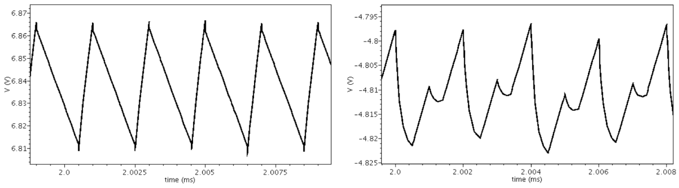

Positive output voltage. Negative output voltage.

(b) Simulation results under condition 4.

Fig. 4. Transient responses using the proposed timing diagram.

TABLE II
OUTPUT VOLTAGE AND ITS RIPPLE VOLTAGE

	output voltage (positive)	ripple (positive)	output voltage (negative)	ripple (negative)
Condition 1 (Conventional)	6.9V	75.5mV	-5.9V	54.3mV
Condition 2 (Conventional)	8.2V	95.9mV	-7.2V	69.5mV
Condition 3 (Proposed)	6.8V	56.1mV	-6.0V	27.6mV
Condition 4 (Proposed)	6.8V	56.1mV	-4.8V	22.1mV

averaging equation is found as

$$\frac{d}{dt}\begin{pmatrix} i_L \\ V_{om} \end{pmatrix} = \begin{pmatrix} 0 & -\frac{D_5}{L} \\ \frac{D_4}{C_{om}} & -\frac{D_4+D_5}{R_{om}C_{om}} \end{pmatrix} \begin{pmatrix} i_L \\ V_{om} \end{pmatrix} + \begin{pmatrix} \frac{D_4+D_5}{L} \\ 0 \end{pmatrix} V_{in}, \quad (12)$$

where D_4 and D_5 are duty ratios of "stage 4" and "stage 5" i.e. T_4/T_s and T_5/T_s, respectively. From Eq.(12), the negative output voltage V_{om} is found as

$$V_{om} = -\frac{D_4 + D_5}{D_5} V_{in} + V_F. \quad (13)$$

Eq.(13) indicates that V_{om} can be controlled with the duty ratio D_4 and D_5 and is independent of V_{op}.

III. SIMULATION RESULTS

Simulations are performed to verify the proposed timing diagram using Spectre program. Figure 1(a) is used for verification. Parameters used in the simulations are shown in Table I.

Figures 3 and 4 exhibit transient responses of the converter.

Figures 3(a) and 3(b) show simulation results of transient response using the conventional timing diagram of Fig.1(b). In order to confirm that V_{om} depends on V_{op} as given by Eq.(5), simulations are performed under two conditions. V_{op} and V_{om} using the conventional timing diagram, are obtained from Eqs.(5) and (7). Duty ratio is set to $D_1 = D_2 = 0.4$, i.e. $V_{op} = 7.0$V and $V_{om} = -6.15$V(Condition 1), and $D_1 = 0.35, D_2 = 0.25$, i.e. $V_{op} = 8.4$V and $V_{om} = -7.55$V(Condition 2). We can see from Figs. 3(a) and 3(b) that V_{op} becomes theoretical value and V_{om} varies by V_{op} of Eq.(5).

Figures 4 indicates simulation results using the proposed timing diagram of Fig.2. Theoretical values of V_{op} and V_{om} are obtained from Eqs.(5) and (13). $D_i(i = 1, 2, 4, 5)$ is set to 0.25, 0.24, 0.25, and 0.24, so that we get $V_{op} = 7.0$V, $V_{om} = -6.15$V(Condition 3), and $D_i(i = 1, 2, 4, 5) = 0.25, 0.24, 0.20, 0.30$, $V_{op} = 7.0$V, $V_{om} = -5.0$V(Condition 4). We can see from Figs. 4(a) and 4(b) that V_{op} and V_{om} become theoretical values and V_{op} is constant value for the variation of V_{om}. The output voltage and its ripple voltage of these results are summarised in Tab.II. Simulation results indicate that ripple voltage using the proposed timing diagram is less than that using the conventional one.

Figure 5 shows inductor current under conditions 1 and 3. Solid line and dotted line illustrate the inductor current under condition 1 and 3 respectively. From the simulation results, the inductor current ripple using the proposed timing diagram is obtained as 853.7mA while that using the conventional one 1.37A. This results indicate that the proposed timing diagram

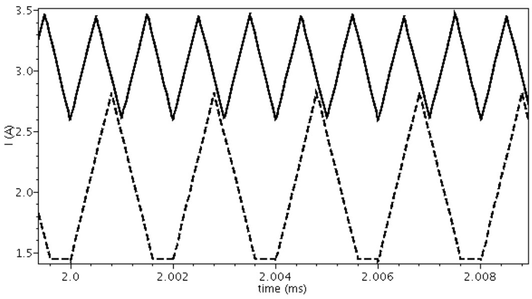

Fig. 5. Inductor current under conditions 1 and 3.

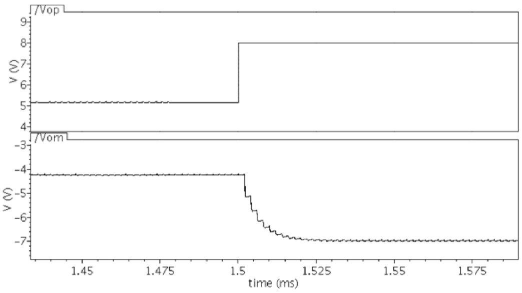

(a) Conventional timing diagram.

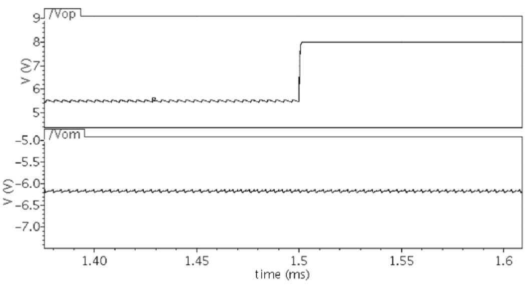

(b) Proposed timing diagram.

Fig. 6. Output response for output voltage variation.

have advantage with respect to the inductor current ripple.

Cross-regulation is very important feature when SIMO is employed. Simulation results of output responses for output voltage variation are shown in Fig. 6. The output voltage is changed from steady-state value of each output voltage to 8V. Figure 6(a) exhibits cross-regulation characteristics using the conventional timing diagram. Because V_{om} is dependent on V_{op}, V_{om} is affected from the variation of V_{op}. Figure 6(b) indicates cross-regulation characteristics using the proposed timing diagram. We can see from 6(b) that V_{om} does not change for the variation of V_{op} and cross-regulation is good performance thanks to PCCM.

Finally, figure 7 shows power efficiency for the variation of load resistance from $R_o = 5\Omega$ to $R_o = 25\Omega$ in steps of 5Ω. The efficiency is defined as (positive output power + negative output power)/(input power). From the simulation results, the efficiency using proposed timing diagram is as same as that using the conventional one.

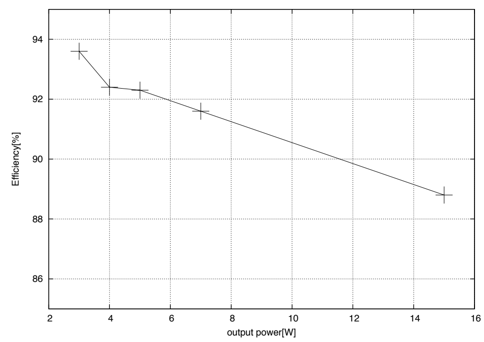

Fig. 7. .

IV. Conclusion

Single inductor DC-DC converter with bipolar outputs using charge pump has been proposed. The conventional timing diagram used in the SIMO converter has problem that the negative output voltage depends upon the positive output voltage. By adding new duty ratio to the conventional timing diagram, bipolar outputs of the proposed timing diagram can be changed independently. Spectre simulation results indicate that the negative output voltage using the proposed timing diagram can be controlled irrespective of the positive output variation while that using the conventional timing diagram depends on the positive output variation. Moreover, output voltage ripple and inductor current ripple using the proposed timing diagram are less than those using the conventional one. Cross-regulation characteristics of the proposed timing diagram is good performance.

References

[1] H.-P. Le, C.-S. Chae, K.-C. Lee, G.-H. Cho, S.-W. Wang, G.-H. Cho, and S. il Kim, "A single-inductor switching DC-DC converter with 5 outputs and ordered power-distributive control," in *Proc. of ISSCC*, no. 29.9, Feb. 2007, pp. 534–535.

[2] C.-S. Chae, H.-P. Le, K.-C. Lee, M.-C. Lee, G.-H. Cho, and G.-H. Cho, "A single-inductor step-up DC-DC switching converter with bipolar outputs for active matrix OLED mobile display panels," in *Proc. of ISSCC*, Feb. 2007, pp. 136–137.

[3] S.-C. Koon, Y.-H. Lam, and W.-H. Ki, "Integrated charge-control single-inductor dual-output step-up/step-down converter," in *Proc. of ISCAS*, May 2005, pp. 3071–3074.

[4] W. Ki and D. Ma, "Single-inductor multiple-output switching converters," in *Proc. of Power Elec. Specialist Conf.*, June 2003.

[5] Z. HU and D. MA, "A pseudo-CCM buck converter with freewheel switching control," in *Proc. of ISCAS*, May 2005, pp. 3083–3086.

[6] Y.-J. Woo, H.-P. Le, G.-H. Cho, G.-H. Cho, and S.-I. Kim, "Load-independent control of switching DC-DC converters with freewheeling current feedback," *IEEE Journal of Solid State Circuit*, vol. 43, no. 12, pp. 2798–2808, December 2008.

[7] D. Ma, W.-H. Ki, and C.-Y. Tsui, "A pseudo-ccm/dcm simo switching converter with freewheel switching," *IEEE Journal of Solid State Circuit*, vol. 38, no. 6, pp. 1007–1014, June 2003.